

An Image Processing approach to identify solar plages observed at 393.37 nm by Kodaikanal Solar Observatory

Sarvesh Gharat,^{1*} Bhaskar Bose² and Abhimanyu Borthakur³

¹ Centre for Machine Intelligence and Data Science, Indian Institute of Technology Bombay, 400076, Mumbai, India

² Smart Mobility Group, Tata Consultancy Services, 560067, Bangalore, India

³ Department of Electronics and Communication Engineering, Manipal Institute of Technology, 576104, Karnataka, India

Accepted XXX. Received YYY; in original form ZZZ

ABSTRACT

Solar Plages are bright chromospheric features observed in Ca II K photographic observations of the sun. These are regions of high magnetic field concentration thus tracer of magnetic activity of the Sun and are one of the most important features to study long term variability of the Sun as Ca II K spectroheliograms are recorded for more than a century. . However, detection of the plages from century-long databases is a non-trivial task and need significant human resources for doing it manually. Hence, in this study we propose an image processing algorithm which can identify solar plages from Ca II K photographic observations. The proposed study has been implemented on archival data from Kodaikanal Solar Observatory. To ensure that the algorithm works, irrespective of noise level, brightness and other image properties, we randomly draw a samples of images from data archive to test our algorithm.

Key words: Sun: chromosphere – Sun: faculae, plages – techniques: image processing

1 INTRODUCTION

Solar Plages are the regions of high magnetic field concentration, which can help in tracing magnetic activity of the Sun (Shine & Linsky 1974) (Azariadis & Guesnerie 1986) (OLSON et al. 1978) (Neidig 1989) (Mackay et al. 2008) (Canfield et al. 2000) (Shine & Linsky 1972). Kodaikanal Solar Observatory has been actively observing Sun in Ca K wavelength since 1907 (Chatterjee et al. 2016) (Hasan et al. 2010), hence generating tremendous amount of data. It is almost impossible for professional solar astronomers to manually identify Solar Plages (Barata et al. 2018) (Benkhalil et al. 2003). Hence, in this study we propose an image processing algorithm to identify plages from Ca II spectroheliograms from Kodaikanal Observatory. The required data for this study has been collected from KSO data archive. To ensure that we cover all sort of images irrespective of varying brightness, noise, contrast and multiple image distortions, we randomly sample 900 + images from data archive.

Previously, lot of study has been done in identifying different solar features including sun spots, plages, filaments, etc (Barata et al. 2018) (Benkhalil et al. 2003) (Aschwanden 2010) (Qahwaji & Colak 2005) (Aboudarham et al. 2008) (Scholl & Habbal 2008). However, there's no exclusive study done for Kodaikonal observatory, hence we find a need to propose an image processing algorithm to automate this process. The data generated from this study along with some modifications can also be used to train a segmentation based algorithm such as U-net.

In (Barata et al. 2018) Barata et. al. make use of morphological transformations to segment data from Coimbra Observatory spectroheliograms. The authors make use of various transformations such

as dilation, erosion and top hat before thresholding. However, considering the variation of data along with varying quality of images from KSO data archive, we can't make use of that algorithm in this case.

In (Benkhalil et al. 2003) Benkhalil et. al. make use of thresholding along with basic morphological operations, similar to (Barata et al. 2018) to detect active regions from Meudon Observatory in H α and Calcium K images. Considering the difference in type of images and generalising for all 3 levels, all these algorithms won't be a good choice to use in case of Kodaikonal Observatory.

In (Aschwanden 2010) the authors provide an extensive review on use of Image Processing to identify different solar features along with the time dependency. The author's have also elaborated on use of Neural Networks to identify different features. However this study is limited to the features, wherein we have large amount of labelled data unlike plages. In (Qahwaji & Colak 2005) Qahwaji and Colak, focus on identification of plages along with providing a classification algorithm to differentiate plages and filaments. The proposed algorithm makes use of morphological classification along with hole filling on data from Meudon Observatory.

Similarly in (Aboudarham et al. 2008) (Scholl & Habbal 2008) the authors make use of different morphological transformations to identify multiple solar features.

However, as discussed earlier due to variation in image properties such as varying brightness, contrasts, artificial artifacts, etc we find a need to propose a novel algorithm to identify plages in generalised images (i.e all 3 levels are covered). We make use of OpenCv (Bradski 2000) to implement the proposed algorithm.

To test our algorithm, we first manually annotate a random sample of images. For the same set of images, using our algorithm's prediction,

* E-mail: sarveshgharat19@gmail.com

we further make use of a popular metric called IOU (Intersection over Union) (Rosebrock 2005) to check our algorithm's efficiency.

2 METHODOLOGY

In this section, we discuss about the methodology used in this paper. The section is divided in following subsections:

1. Data Collection
2. Pre Processing
3. Plages Detection
4. Post Processing

2.1 Data Collection

An important part of any study involving data is the collection of data. In this study, we collect data from KSO data archive.

The collected data comprises of randomly sampled level 0 (raw), 1 (Basic Calibrated) and 2 (Limb Darkening Corrected) images with Ca K filter. More information on level of images can be viewed on official website of KSO data archive (<https://kso.iap.res.in/new/data>). In Figure 1, we show one image from level 0, 1 and 2 respectively

The collected data is further pre-processed using multiple image processing algorithms before identifying plages. However, due to presence on uneven brightness, there are many outliers which are mistaken as plages. Hence to remove those, use of multiple post-processing techniques happens to be must. A detailed description on these techniques is discussed in further subsections.

2.2 Pre Processing

In Algorithm 1, we provide a rough overview on steps followed in this subsection. We also provide a theoretical summary and importance of every step used in this algorithm as mentioned in subsequent sub subsections.

Algorithm 1 : Pre Processing

- 1: Start
 - 2: **while** Images are present **do**
 - 3: Median Blur with Kernel Size 3
 - 4: Image conversion to B/W image
 - 5: CLAHE with clip limit 3
 - 6: 2 Iterations of Erosion
 - 7: 1 Iteration of Dilation
 - 8: **end while**
 - 9: Stop
-

2.2.1 Median Blur

The data, due to increase in resolution and varying brightness level has a wide component of salt and pepper noise. Hence, to remove the same, we make use of median blur (Arce & McLoughlin 1987). Kernel Size (Horiuchi et al. 2019) acts as an important hyper parameter contributing to reduction of noise. Hence, to tune this hyper parameter we make use of hit and trial method. This filter is similar to other averaging filters. However, unlike average filters here we replace central pixel of kernel by median of pixels in the kernel area.

Figure 2 represents the output of median blur on input images as shown in Figure 1.

2.2.2 CLAHE

Histogram equalization (Pizer et al. 1987) is one of the most popular and widely used technique to improve contrast of any image (Abdullah-Al-Wadud et al. 2007). As pixel intensities surrounding the plages are not consistent, along with varying uneven brightness, use of global histogram equalization techniques is not possible. Hence in this study, we make use of Contrast Limited Adaptive Histogram Equalization (CLAHE) (Reza 2004) which extends the original technique by focusing separately on different regions within the image. Additionally, a clipping factor (Sundaram et al. 2011) (Liu et al. 2019) is also defined that clips the histogram at a certain point which prevents the over-amplification of noise as seen with a previous version. This clipping factor is one of the parameters that needs to be experimentally tuned to give the best possible results.

In Figure 3, we see the output after applying CLAHE on Figure 2 with clip factor of 3.

2.2.3 Erosion and Dilation

Erosion and Dilation (Soille 2004) are the basic transforms particularly used to enhance and remove small contrasting spots. Erosion is mainly responsible for removing the regions which are smaller than structuring element. Similarly, dilation joins two regions wherein the distance between those is less than or equal to structuring element. In this algorithm, erosion and dilation plays an important role in noise reduction. The structuring element here is decided as $k \times \text{number of pixels}$ wherein k is some constant. This step reduces the noise by ensuring that, all the dark pixels surrounded by bright pixels with distance less than that of structuring element are brightened out. Similarly it also removes all the bright pixels whose area is less than that of structuring element.

In Figure 4, we see the output on applying Morphological transformations i.e 2 iterations of erosion and 1 iteration of dilation on output of CLAHE generated images.

2.3 Plages Detection

Algorithm 2 describes the steps followed in this subsection. Here, we ensure that the plages are appropriately detected. On thresholding, along with plages, many outliers due to uneven brightness level are segmented which can result into falsified identification. Hence, to reduce these unnecessary segmented artifacts, we make use of outlier removal techniques (particularly z score). In this subsection, we further discuss more on thresholding and outlier detection technique.

Algorithm 2 : Plages Detection

- 1: Start
 - 2: **while** Images are present **do**
 - 3: Thresholding with threshold of 180
 - 4: 1 Iteration of Erosion
 - 5: 1 Iteration of Dilation
 - 6: Find area of every bright spot
 - 7: Outlier Removal
 - 8: **end while**
 - 9: Stop
-

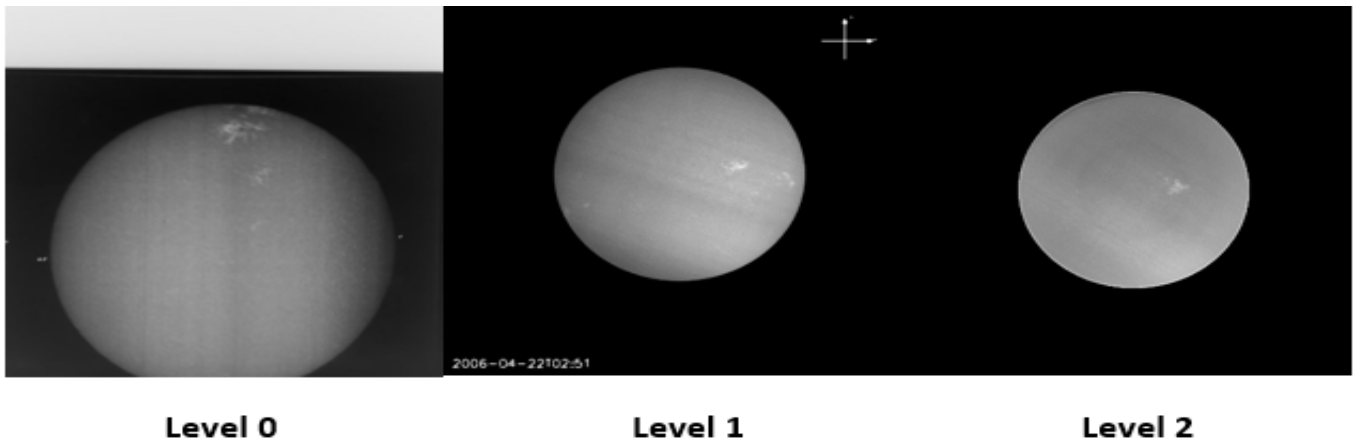


Figure 1. Input images

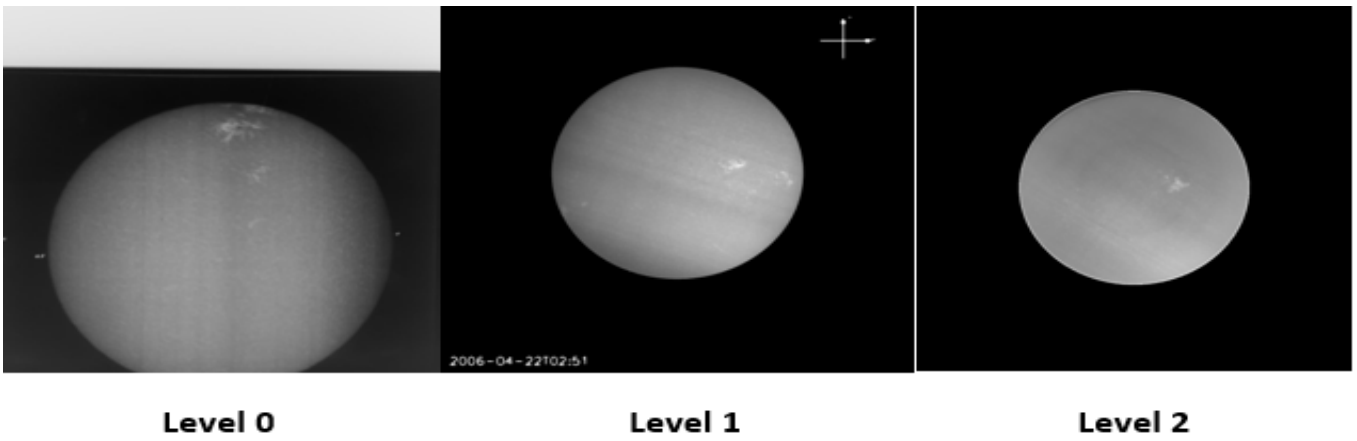


Figure 2. Output of Median Blur

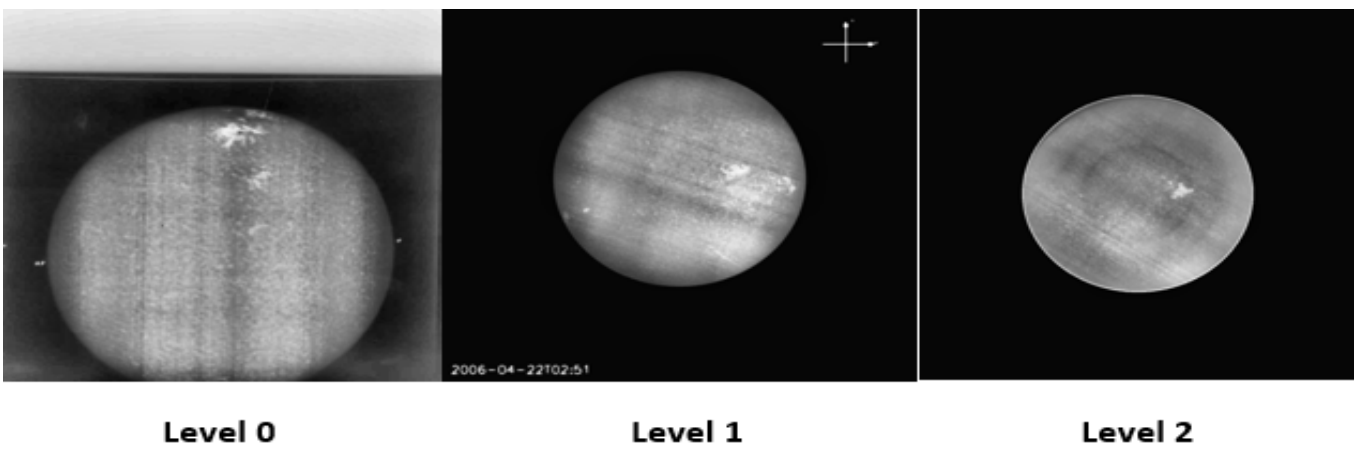


Figure 3. Output of CLAHE

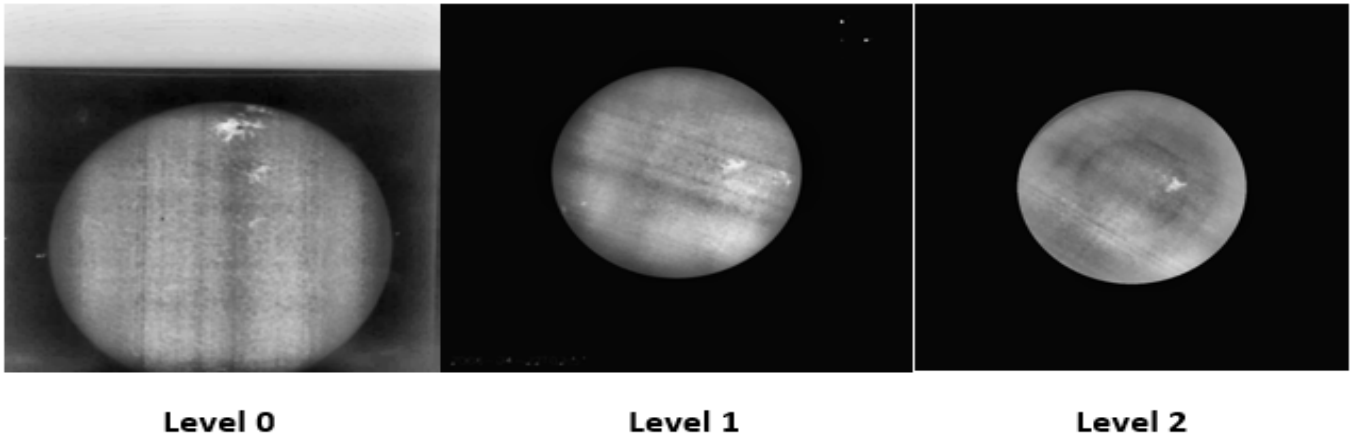


Figure 4. Output after doing Morphological transformation

2.3.1 Thresholding

Image thresholding (Chowdhury & Little 1995) plays an important role in identifying plages. Using this technique, we segment the image by replacing all the pixel values greater than threshold with 255 and 0 for those less than threshold.

In our case, the threshold used is 180. A constant value of threshold works due to use of CLAHE (Reza 2004) which is one of the local histogram equalization technique as stated in previous subsection. Please refer Algorithm 3 to get a rough idea on how the algorithm works.

Algorithm 3 : Thresholding

```

1: Start
2: threshold = 180
3: for pixel in image do
4:   if pixel value > threshold then
5:     pixel value = 255
6:   else
7:     pixel value = 0
8:   end if
9: end for
10: Stop

```

The output of thresholding can be seen in Figure 5. As seen from the images, even after using multiple pre processing techniques along with morphological transformations as used in multiple published algorithms, there is large amount of noise component involved in these images. Hence, to remove the same we first make use of outlier detection technique, before moving to post processing.

2.3.2 Outlier detection

After thresholding and performing basic transformations (erosion and dilation), we get our segmented image. However due to artificial artifacts such as uneven bright spots, even these regions are segmented and can be misidentified as plages. Hence, to avoid this outliers (Ben-Gal 2005) we make use of Z-score (Aggarwal et al. 2019). In this method we first calculate area of all plages. Further based on mean and standard deviation of area of plages, we remove the regions which don't satisfy 3σ criteria. Hence, it ends up removing these outliers.

However, this technique can only remove large outliers beyond a certain threshold. Hence, we find a need to make use of post processing techniques to remove all the artifacts having lesser area than threshold.

From Figure 5 and Figure 6 we see that using of outlier detection technique helps us in removing larger noise components as opposed to smaller noise components as discussed earlier.

2.4 Post Processing

As discussed earlier, the smaller artifacts are present even after using outlier removal techniques, hence we need to introduce post processing techniques as mentioned in Algorithm 4

Algorithm 4 : Post Processing

```

1: Start
2: while Images are present do
3:   Perform canny edge detection on Output of CLAHE with
   lower and upper threshold 120 and 250 respectively
4:   Find all contours within the solar circumference
5:   Draw and fill obtained contours in a new blank 2D array 'M'
6:   AND operation between 'M' and output of Algorithm 2
7: end while
8: Stop

```

In this subsection, further we elaborate of Canny Edge Detection and Bit wise AND operator which happens to be an important component in this post processing algorithm.

2.4.1 Canny Edge Detection

Canny Edge detection (Rong et al. 2014) is widely used to extract high frequency features like edges. Use of Canny Edge Detection after CLAHE, helps us in plotting contours on the image which basically covers the region of solar plages along with some noise factor in it. These contours are further stored in a 2D array for further purposes.

As seen from Figure 7, use of Canny Edge detection helps us in identifying contours as observed in Figure 8. However, even these contours have large amount of artifacts present in it. However these artifacts have larger area as opposed to what we saw in Figure 6.



Figure 5. Output after applying thresholding



Figure 6. Output after removing outliers

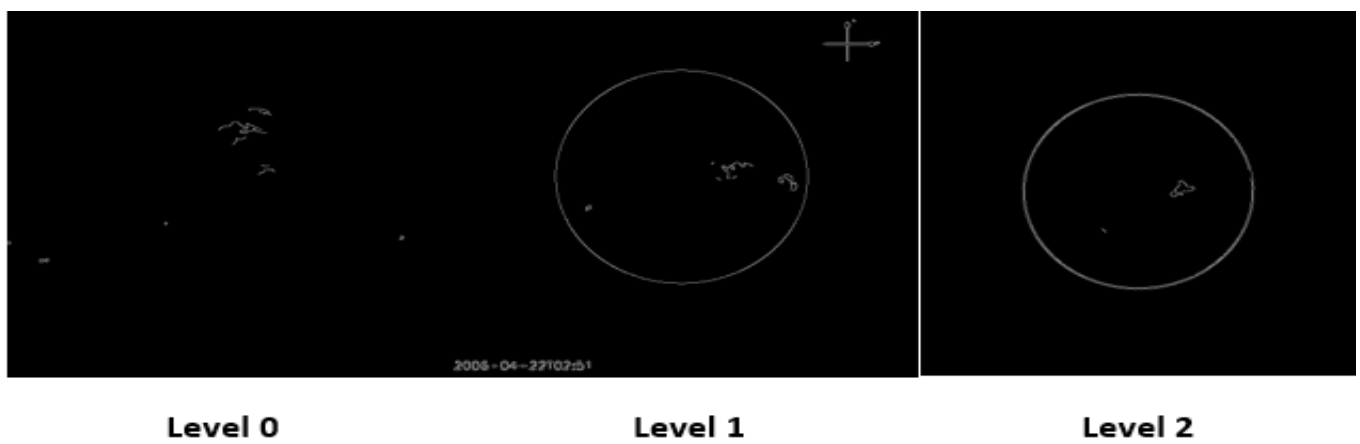


Figure 7. Output after applying Canny Edge detection on output of Figure 3



Figure 8. Contours plotted on blank 2D array

Hence, using of "Bitwise AND operator" helps us in removing major component of noise.

2.4.2 Bitwise AND operator

We make use of "Bitwise AND Operator" (Dmitrović 2021) between output of Algorithm 2 to find intersection between both the arrays. This ensures removal of small level artifacts which was an important concern. Considering bit size to be 8 bit, all the bright pixels will have value of "11111111". Similarly, all dark pixels have value of "00000000". As both the images either have dark or bright pixels, their corresponding pixel values are "00000000" and "11111111" respectively. Hence, using AND operator ensures that the pixel will be bright only if the value of corresponding pixel is 255 in both the images.

In Figure 9, we see the final output images which are generated after taking Bitwise AND operation between Figure 6 and Figure 8. In final image as generated by our algorithm, we see that the algorithm has successfully segmented the plages along with little to no noise component in segmented image.

3 RESULTS AND DISCUSSION

All the previous studies done on automatic identification of solar features fail to work on KSO data archive due to large amount of noise factor and artifacts present in these images (Barata et al. 2018) (Benkhalil et al. 2003) (Aschwanden 2010) (Qahwaji & Colak 2005) (Aboudarham et al. 2008) (Scholl & Habbal 2008). Hence, in this study, we provide a generalised algorithm which can identify plages. To evaluate our model, we manually annotate a random sample of images and ask our algorithm to predict plages for same set of images. Further, we make use of IOU metric (Intersection over Union) to evaluate our model.

In Figure 10, we have input data, and the corresponding output from Algorithm 2 and Algorithm 4 for all 3 levels of images. From Figure 10, we see that the $\text{IOU}(\text{Post Processed}) \geq \text{IOU}(\text{Outlier removal}) \geq \text{IOU}(\text{Thresholded})$. The percentage increase in this value for all level of images is more than 100% for post processed images compared to one's without post processing. This shows an important

reason to have post processing techniques to appropriately detect solar plages. We also see a monotonically increasing function of IOU values as a function of level of images. This is due to initial reduction of noise as discussed in Section 2.1.

In Figures 11, 12 and 13, we show best outputs of randomly sampled 10 images generated from previously published algorithms and compare it with output of our algorithm. As seen from Figures, we observe that our algorithm performs way better on these images compared to that of previously published algorithms. Majority of artificial artifacts present due to uneven brightness, contrast, etc are mistakenly identified as plages by all the published algorithms as opposed to ours which provides a segmented plages image by removing the potential noise.

4 CONCLUSION

In this study, we propose a novel algorithm to identify solar plages from KSO data archive. The proposed algorithm is a generalised algorithm which works on all levels of images as mentioned in the data archive. The algorithm detects the number of plages with very high accuracy (visually compared from input and output images), however when it comes to area of plages the algorithm performs well on level 2 images as compared to level 0 and level 1. The segmented images as generated using our algorithm, also happens to be the best output as compared to output of other published algorithms.

ACKNOWLEDGEMENTS

We want to thank Kodaikanal solar observatory, a facility of Indian Institute of Astrophysics, Bangalore, India for making the archival data available. This data is available for public use at <http://kso.iap.res.in> through a service developed at IUCAA under the Data Driven Initiatives project funded by the National Knowledge Network

DATA AVAILABILITY

The input data used in this study is freely available in KSO data archive.



Figure 9. Output Images

All the codes, used in this study are made available in our GitHub repository (<https://github.com/SarveshVGharat/Plages-Identification>).

REFERENCES

- Abdullah-Al-Wadud M., Kabir M. H., Dewan M. A. A., Chae O., 2007, *IEEE Transactions on Consumer Electronics*, 53, 593
- Aboudarham J., Scholl I., Fuller N., Fouesneau M., Galametz M., Gonon F., Maire A., Leroy Y., 2008, in *Annales Geophysicae*. pp 243–248
- Aggarwal V., Gupta V., Singh P., Sharma K., Sharma N., 2019, in 2019 3rd International Conference on Trends in Electronics and Informatics (ICOEI). pp 788–790
- Arce G., McLoughlin M., 1987, *IEEE transactions on acoustics, speech, and signal processing*, 35, 60
- Aschwanden M. J., 2010, *Solar Physics*, 262, 235
- Azariadis C., Guesnerie R., 1986, *The review of economic studies*, 53, 725
- Barata T., Carvalho S., Dorotovič I., Pinheiro F. J., Garcia A., Fernandes J., Lourenço A. M., 2018, *Astronomy and Computing*, 24, 70
- Ben-Gal I., 2005, in *Data mining and knowledge discovery handbook*. Springer, pp 131–146
- Benkhalil A., Zharkova V., Ipson S., Zharkov S., 2003, in *Proceedings of the AISB*. pp 66–73
- Bradski G., 2000, *Dr. Dobb's Journal of Software Tools*
- Canfield R. C., Hudson H. S., Pevtsov A. A., 2000, *IEEE transactions on plasma science*, 28, 1786
- Chatterjee S., Banerjee D., Ravindra B., 2016, *The Astrophysical Journal*, 827, 87
- Chowdhury M. H., Little W. D., 1995, in *IEEE pacific Rim conference on communications, computers, and signal processing. Proceedings*. pp 585–589
- Dmitrović S., 2021, in *Modern C for Absolute Beginners*. Springer, pp 325–331
- Hasan S., Mallik D., Bagare S., Rajaguru S., 2010, in *Magnetic Coupling between the Interior and Atmosphere of the Sun*. Springer, pp 12–36
- Horiuchi K., Jiang W., Yamagishi S., Zhang X., 2019, in *International Workshop on Advanced Image Technology (IWAIT) 2019*. pp 7–12
- Liu C., Sui X., Liu Y., Kuang X., Gu G., Chen Q., 2019, *Journal of Modern Optics*, 66, 1590
- Mackay D. H., Gaizauskas V., Yeates A. R., 2008, *Solar Physics*, 248, 51
- Neidig D. F., 1989, in *Solar and Stellar Flares*. Springer, pp 261–269
- OLSON R. H., ROBERTS W. O., PRINCE H. D., HEDEMAN E., 1978, *Nature*, 274, 140
- Pizer S. M., et al., 1987, *Computer vision, graphics, and image processing*, 39, 355
- Qahwaji R., Colak T., 2005, *International Journal of Imaging Systems and Technology*, 15, 199
- Reza A. M., 2004, *Journal of VLSI signal processing systems for signal, image and video technology*, 38, 35
- Rong W., Li Z., Zhang W., Sun L., 2014, in *2014 IEEE international conference on mechatronics and automation*. pp 577–582
- Rosebrock A., 2005, URL <https://www.pyimagesearch.com/2016/11/07/intersection-over-union-iou-for-object-detection>
- Scholl I. F., Habbal S. R., 2008, *Solar Physics*, 248, 425
- Shine R. A., Linsky J. L., 1972, *Solar Physics*, 25, 357
- Shine R. A., Linsky J. L., 1974, *Solar Physics*, 39, 49
- Soille P., 2004, in *Morphological Image Analysis*. Springer, pp 63–103
- Sundaram M., Ramar K., Arumugam N., Prabin G., 2011, in *2011 International conference on signal processing, communication, computing and networking technologies*. pp 842–846

This paper has been typeset from a \LaTeX file prepared by the author.

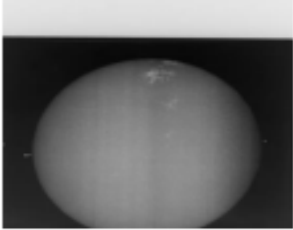



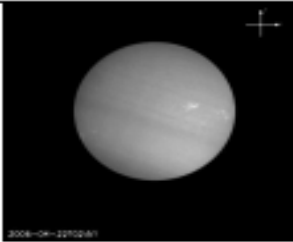

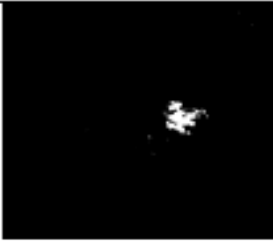

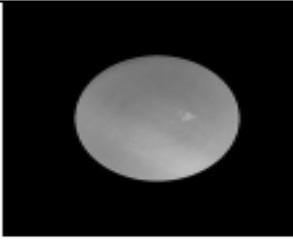


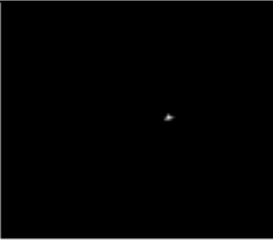
| INPUT | GROUND TRUTH | OUTPUT (WITHOUT POST- PROCESSING) | OUTPUT (WITH POST- PROCESSING) |
|---|---|--|--|
|  LEVEL 0 |  |  IOU: 0.162(after outlier removal) 0.009(prior to outlier removal) |  IOU: 0.264 |
|  LEVEL 1 |  |  IOU: 0.081(after outlier removal) 0.034(prior to outlier removal) |  IOU: 0.346 |
|  LEVEL 2 |  |  IOU: 0.163(after outlier removal) 0.059(prior to outlier removal) |  IOU: 0.432 |

Figure 10. Comparison of manually annotated, output of Algorithm 2 and output of Algorithm 4 images

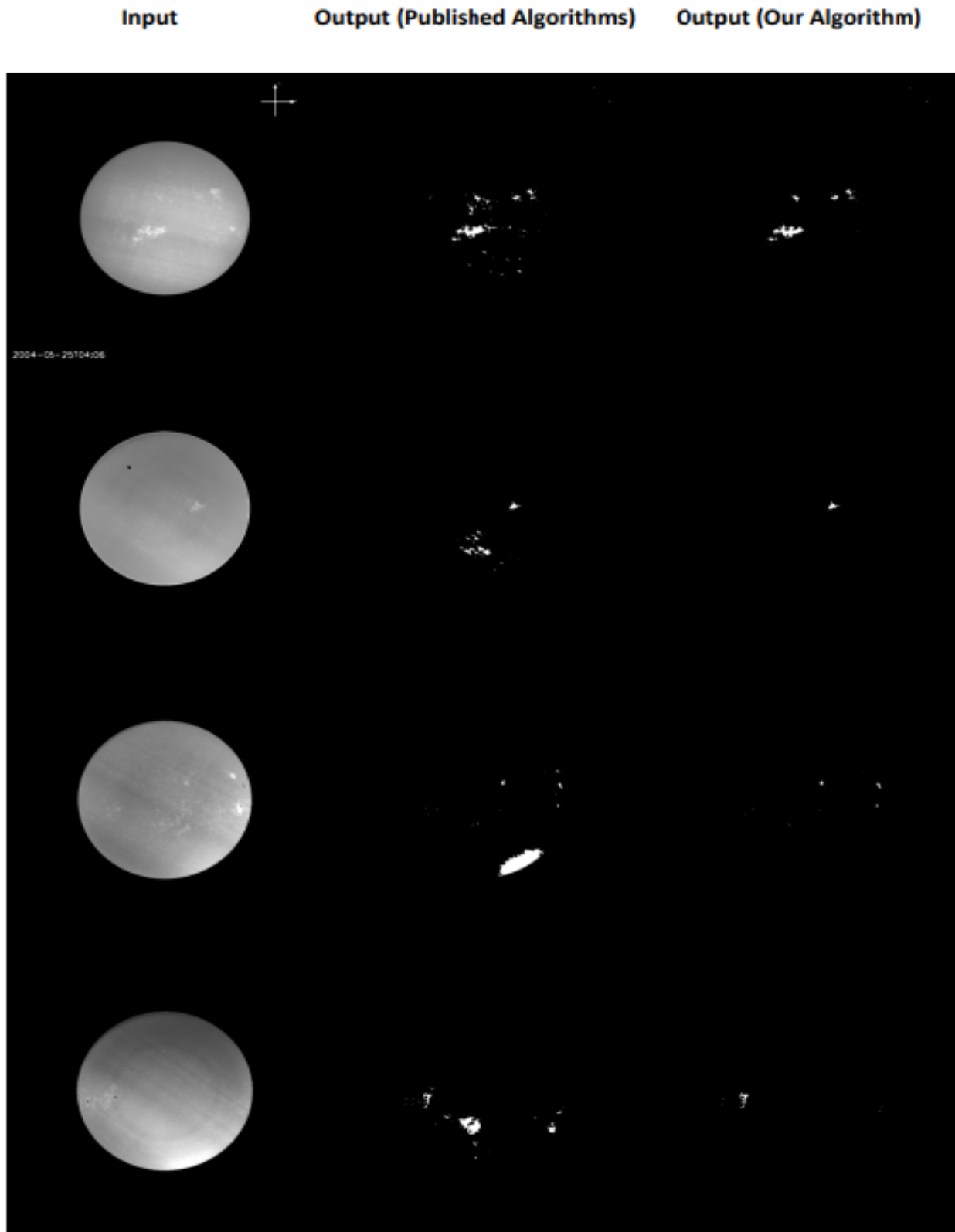


Figure 11. Comparison between best output of published algorithms ([Barata et al. 2018](#)) ([Benkhalil et al. 2003](#)) ([Aschwanden 2010](#)) ([Qahwaji & Colak 2005](#)) ([Aboudarham et al. 2008](#)) ([Scholl & Habbal 2008](#)) and our Algorithm

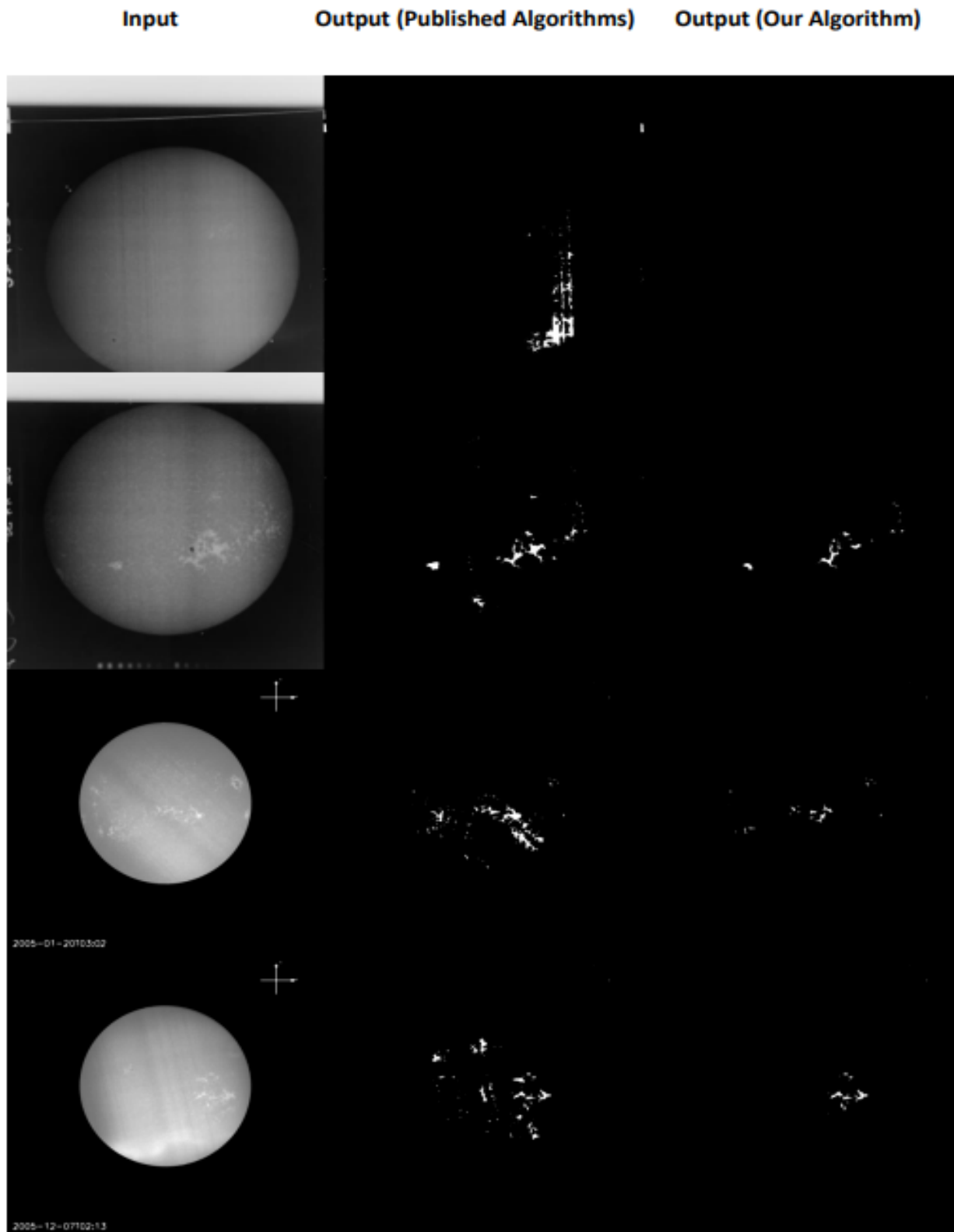


Figure 12. Comparison between best output of published algorithms ([Barata et al. 2018](#)) ([Benkhalil et al. 2003](#)) ([Aschwanden 2010](#)) ([Qahwaji & Colak 2005](#)) ([Aboudarham et al. 2008](#)) ([Scholl & Habbal 2008](#)) and our Algorithm

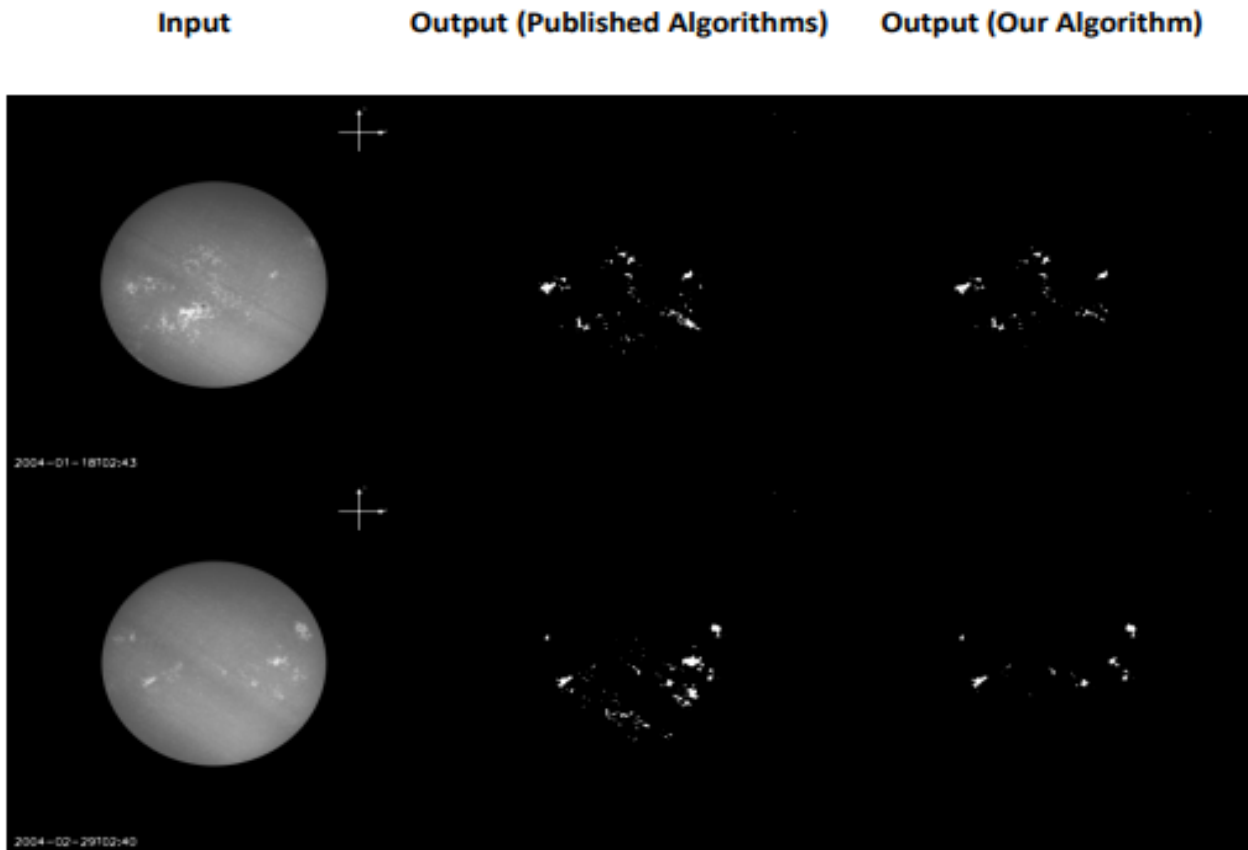


Figure 13. Comparison between best output of published algorithms ([Barata et al. 2018](#)) ([Benkhalil et al. 2003](#)) ([Aschwanden 2010](#)) ([Qahwaji & Colak 2005](#)) ([Aboudarham et al. 2008](#)) ([Scholl & Habbal 2008](#)) and our Algorithm